NEW DEVELOPMENTS AND APPLICATIONS IN SOL-GEL COATINGS

M.A. Aegerter
Institut für Neue Materialien
Department of Coating Technologies
Im Stadtwald, Gebäude 43 a
66123 Saarbrücken, Germany

ABSTRACT

In this overview we describe some recent developments of technological interest realized at INM in the processing of sol-gel coatings. Nanoscale crystalline particles, fully redispersed in aqueous solutions, have been developed to produce thin ceramic layers at low temperature. As an example, antistatic optical coatings and conducting membranes based on SnO_2:Sb material are reported. New wet chemical processes have been developed to extend the sol-gel basic principles for the coating of oxide compounds on plastic (biomimetic process) and sulfide materials (MoS_2). Also ink-jet and pad printing processes, well established in other fields, have been adapted for the development of micro structured coatings. As examples, the realization of single and arrays of spherical and cylindrical refractive microlenses is presented. Finally non conventional sintering process using high power CO_2 laser is exemplified for the obtention of optical quality transparent conducting coatings under high sintering rate(30 cm^2/s).

INTRODUCTION

Most of the interest in sol-gel synthesis for thin film deposition was concentrated in the past years on the hydrolysis of alkoxides in organic solvent. Many single or multi components oxide coatings have been obtained using essentially the dip and spin coating processes and characterized but, in spite of the great success obtained in the laboratories, only a few systems are presently used on a commercial basis as the industry still gives a preference to more conventional deposition techniques such as sputtering, physical and chemical vapor deposition, etc. Consequently several issues are of technological interest at present.

In this paper we briefly report on some recent developments realized at the Institut für Neue Materialien - INM to fulfill some of these issues. The use of alcoholic solvents is sometimes considered as a drawback of the method and alternative sol-gel processes using aqueous media can often be just as useful and we show that narrow sized nanocrystaline sol-gel powders fully redispersable in aqueous media can be used to obtain optical quality coatings. The case of SnO_2:Sb is exemplified for the development of antistatic coating and conducting membranes for ultra filtration [1,2,3]. The sol-gel process has been essentially developed for oxide materials and wet chemical processes allowing the use of the simple and inexpensive dip or spin coating techniques of non-oxide materials have not been systematically investigated so far. The development of wet chemical processes using single source non-oxide precursor is then reported. The technique has been successfully applied to obtain thin MoS_2 layers using the spin coating process [4]. New coating deposition techniques are also discussed. The ink-jet and pad printing processes have been developed to deposit structural coatings and optical micro components using hybrid inorganic-organic sols [5,6] while the biomimetic approach is shown to be of interest to deposit hydrated TiO_2 thin films on polycarbonate substrate [7,8]. Finally the use of high power CO_2 laser is exemplified as a non conventional high rate sintering process to obtain transparent conduction SnO_2:Sb coating of high optical quality [9].

COATING OBTAINED WITH REDISPERSABLE NANOCRYSTALLINE PARTICLES [1-3]

The application of the sol-gel methods based on the well known hydrolysis-polycondensation processes using metal alkoxides or oxoalkoxides based sols results after deposition to wet and usually amorphous coatings whose composition reflects a complex structure where the metal ion is linked to anionic ligand (alkoxide, acetate, OH, Cl etc.). The organic content is then burnt by heating at 300 - 500°C and at the same time the coatings densify and in most cases crystallize. A complete densification is however never obtained (or obtained at very high temperature) and the sol-gel layers are usually more porous than those obtained by other deposition process (CVD, sputtering, PVD, etc.). The preparation of coatings using already dense crystalline nano particles with a controlled size is therefore an interesting issue which may lead to coatings presenting higher densitiy and better crystallinity after treatment at a lower sintering temperature. This requires the availability of sols loaded with fully redispersable nanocrystalline particles which can then be processed by the now conventional spin or dip coating techniques. The nanosize of the precursor components will also be a warranty to obtain high optical quality coating presenting low light scattering.

As an example SnO_2:Sb nanoscale powders have been prepared by a controlled growth technique [1,10, 11]. A solution of tin (IV) chloride in ethanol containing 0.1 - 10 mole % of $SbCl_3$ (dopant) was added drop-wise to an aqueous ammonia solution containing 10 wt% of a surface modifying agent, ß-alanine. The prepared suspensions were hydrothermally treated at 150°C under a 3 bar pressure for 3 h.The resulting powder was isolated by centrifuging and washed with water several times and then dried at 60°C. The powders consist of crystalline particles (cassiterite structure) with average particle size of 3-5 nm without evidence of aggregation. These particles can be fully redispersed in water at pH > 11 under ultrasound using tetramethylammoniumhydroxide as dispersing agent [1,2] with solid content up to 50 mass%.

Deposition by spin coating (2000 rpm) results to coating whose thickness increases exponentially with the concentration (typically from ~ 100 nm for a 2.5 mass% to 225 nm for a 26 mass% . The electrical specific resistivity of single SnO_2:Sb layer heat treated at 550°C for 15 min. decreases with the particle concentration from 10 Ωcm (2.5 mass%) down to a minimum value of ~ 4.2 10^{-2} Ωcm for a particulated sol with 26 mass%. Higher concentration leads to cracks in the coatings increasing the resistivity. These values are unfortunately still higher than those obtained with a conventional sol-gel process, typically 2 10^{-3} Ωcm [12] or prepared by spray pyrolysis ($\rho \cong 9\ 10^{-4}$ Ωcm) [13]. The coatings are highly transparent in the visible spectral range with transmission as high as 92% and present interesting antistatic and optical properties.

The BET surface and density (measured by He picnometry) of the powders processed in air at different temperatures and sintering times is shown in figure 1. Particles with the density close to the theoretical density (~ 7g /cm^3) can only be obtained at high temperature (T> 600°C) after long sintering time (300 min).

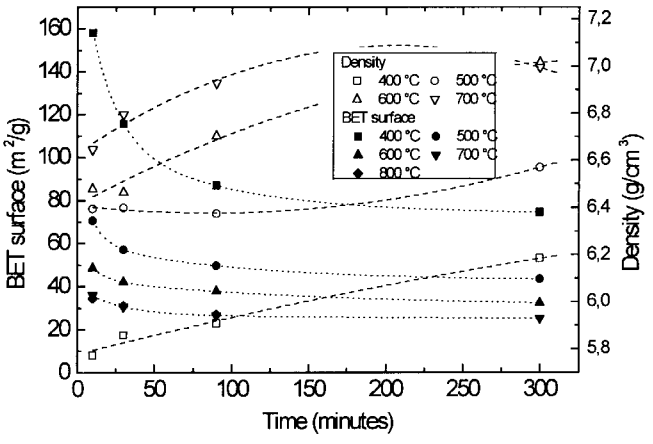

Fig. 1: Influence of temperature and sintering time on the BET surface and the density of SnO_2:Sb powder

At temperature and time normally used to sinter coating on float or borosilicate glass the particle density is 10% smaller. The pore characteristics (volume, size) of these powders under the same treatments are shown in figure 2. The average pore diameter can be adjusted from ≤ 4 nm to ~ 20 nm by varying the sintering conditions. The pore distribution is very narrow (± 1nm at 400°C, ± 2nm at 800°C) and the maximum pore volume constant (~0.75 cm^3/g). As these particles can be deposited into crack free layers by spin coating (200 nm for 1 layer, with the possibility to increase the thickness by repeating the coating process [14]), such a process turns out quite interesting for the development of conducting ultrafiltration membranes [3].

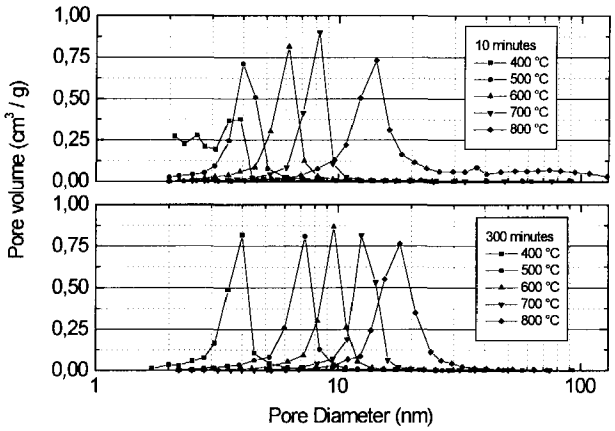

Fig. 2: Evolution of pore characteristics (volume, size) with sintering temperature and time

SPIN COATING OF THIN SULFIDE COATINGS [4]

Various deposition techniques have been used for the preparation of sulfide films among which the physical and chemical vapor deposition, chemical bath deposition, electric deposition are the most important. Wet chemical processes allowing for simple and inexpensive spin coating process have so far not been explored. First results for the deposition of sulfides form different precursor solutions have been however reported for amorphous As_2S_3 [15,16,17] and As_2Se_3 [18], but similar attempts for the preparation of Sb_2S_3 and GeS_x have not been successful [17].

We have developed a different approach in which a sulfide salt dissolved in an organic solvent allows to obtain a spinnable solution which wets the substrate and where the solvent can be removed by a thermolysis process. MoS_2 thin films have been successfully obtained in this way by dissolving $(NH_4)_2MoS_4$ in an organic diamine [4]) such as 1,2-diaminoethane [en], 1,2-diaminopropane [12dap] or 1,3-diaminopropane [13dap]. During the reaction NH_3 is released briskly under formation of the corresponding diammonium salt $[H_3N\text{-}C_nH_n\text{-}NH_3]MoS_4$ leading to deep red solutions. Thin film deposited by spin coating technique at 2000 rpm during 1min on fused silica substrates are orange in color and turn red-brown after a drying step at 250°C in air due to the thermolysis of the diammonium salt during the formation of amorphous MoS_3. Under further thermolysis at temperatures between 600 and 800°C during 1 h under N_2 atmosphere, MoS_3 slowly decomposes into MoS_2 and sulfur and deep brown highly reflective crystalline films, 90 to 150 nm thick, are obtained. X-ray diffraction of $[enH_2]MoS_4$ based films, heat treated at T>600°C shows only one peak at $2\theta \cong 14°$ corresponding to the (002) plane (Fig.3). The coatings are poorly crystalline and a careful analysis indicates that they are made of MoS_2 layer fragments essentially oriented with their basal planes parallel to the surface corresponding to a type II coating [19]. A high resolution transmission electron microscopy analysis reveals that these fragments have an average length between 5 and 10 nm and an average number of layers in each stack between 1 and 3. Between the small crystallites more or less amorphous areas are visible (Fig.4). $[12dapH_2]MoS_4$ based films show a different structure where the 2θ (002) peak is slightly shifted to a lower angle and an additional broad 2θ peak which cannot be indexed to any of the known molybdenum sulfides appears at 10.5°. HRTEM images reveal that the fragments are mostly two layered stacks bent in direction of the c-axis with an

increased space between the basal planes due to the occurrence of fork or dislocation defects (insertion of additional layers) or the intercalation of foreign molecules.

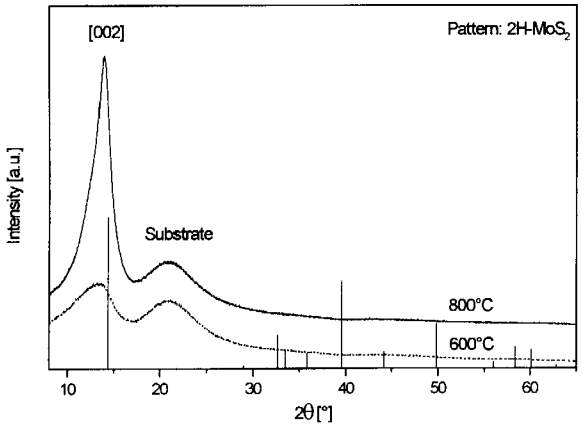

Fig.3: XRD of MoS_2 films prepared from 0.5 M solutions of $(NH_4)_2MoS_4$ in 1,2-diaminoethane after heat treatment at temperatures of 600 - 800°C for 1 h

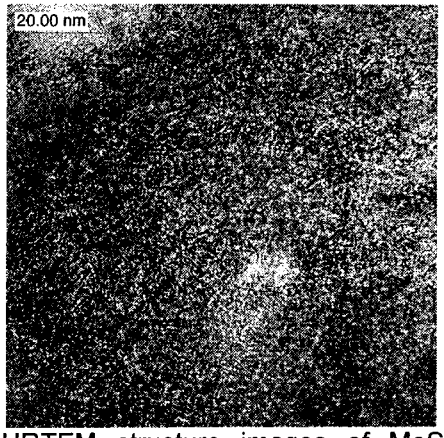

Fig.4: HRTEM structure images of MoS_2 films prepared from 0.5 M solutions of $(NH_4)_2MoS_4$ in 1,2-diaminoethane after heat treatment at a temperature of 600°C for 1 h

The optical spectra of films prepared from solutions of $(NH_4)_2MoS_4$ in 1,2-diaminoethane, 1,2-diaminopropane, and 1,3-diaminopropane after heat treatment at a temperature of 600°C for 1 h are shown in figure 5. The coatings are brown in transmission with a reflection between 30 and 40% in the visible range of the spectrum.

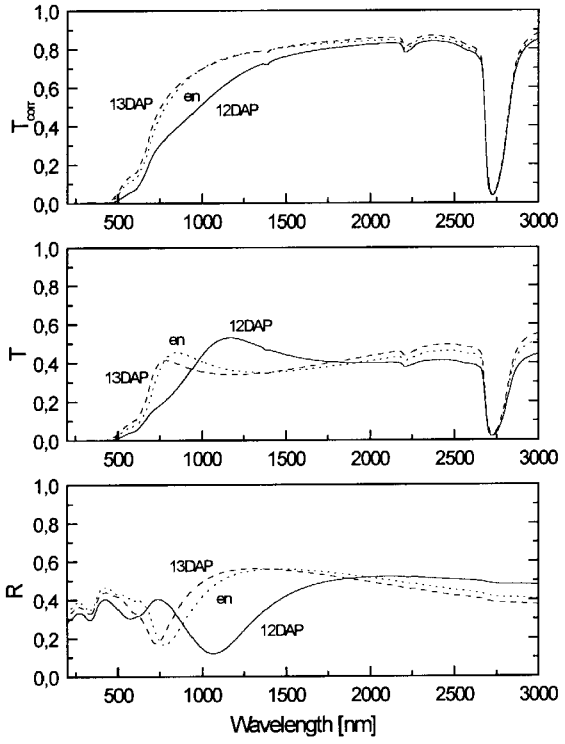

Fig.5: Optical spectra of films prepared from solutions of $(NH_4)_2MoS_4$ in 1,2-diaminoethane (en), 1,2-diaminopropane (12dap) and 1,3-diaminopropane (13dap) after heat treatment at 600°C for 1 h in N_2

From the corrected transmission T_{corr} the high absorption $A = 1-T_{corr}$ in the range from 200 to 600 nm becomes evident. The absorption coefficient at 550 nm α_{550} is about 2×10^5 cm^{-1}. From a plot of α^2 and $\alpha^{0.5}$ vs. the energy the direct and indirect band gap were determined as 1.80 ± 0.02 eV and 1.20 ± 0.05 eV, respectively. These values are in good agreement with band gaps obtained with other deposition techniques and for bulk MoS_2. Differences in the optical spectra for 1,2-diaminoethane and 1,3-diaminopropane on the one side and for 1,2-diaminopropane on the other side may arise from the different degree of crystallinity of the samples. The strong absorption at ca. 2700 nm can be attributed to Si-OH vibrational modes in the substrate.

The development of wet chemical preparation reported here for the obtention of high optical quality MoS_2 thin film by the spin coating technique opens new possibilities for the development of chalcogenide based coatings.

INK-JET AND PAD PRINTING OF Si BASED HYBRID COATINGS

Sol-gel coatings are usually obtained by dip and spin coating technique. Patterning of these coatings is possible and techniques such as laser ablation, UV (lamp or excimer laser) irradiation or embossing have been used. It exists however on the market printing equipments which allow to print patterns on substrates.

The ink-jet process is of common use in computer controlled printing [20]. To our knowledge sol-gel based inks have been only recently proposed to decorate ceramic tiles using a continuous process [21] and for the realization of spherical microlenses [22]. The pad printing is widely used in the industry to print small flat or curved substrates [23] but, to our knowledge, no sol-gel based ink have been yet developed. Such technologies have been used to manufacture microlenses on glass substrates using sols prepared Iron hybrid organic-inorganic materials.

Using a commercial drop-on-demand ink-jet-equipment (Microdrop SP-K 130), spherical droplets, typically 50 µm in diameter, have been deposited on clean glass substrates and glass substrates coated with a thin layer of a low surface energy perfluorated polymer (FTS/TEOS/MPTS/2-Propanol/Irgacure 184) [24] in order to vary the drop/ substrate wetting conditions. Hybrid organic -inorganic sols have been prepared by hydrolysis of methacryloxypropyltrimethoxysilane (MPTS) mixed with an ethanolic solution of tetraethyleneglycoldimetacrylate (TEGDMA) and a 1 to 10 wt.-% UV photoinitiator (Irgacure 184). They have a typical kinematic viscosity η =3 mm^2/s at 20°C. After deposition, the drops have been polymerized by a 17.5 J/cm^2 UV light irradiation (Kombistrahler Beltron) within 200 s [22]. The deposited material is practically transparent ($T \cong 91\%$) in the 375 nm $< \lambda <$ 2.7 µm region and therefore adequate for the preparation of refractive lenses. Sols having a too high ethanol amount (>40 wt.-%) wet the glass substrate and spreads on it. The inorganic-organic material is transported to the border of the drop and creates a ring shape lens due capillary effect [22]. Sols containing an ethanol fraction smaller than 30 wt-% have a high viscosity $\eta > 5$ mm^2/s, and tend to block the piezoelectric nozzle.

Spherical lens formation was obtained on glass substrate with 30 wt.-% ethanol fraction with a mixture of 50 mol-% TEGDMA (fig. 6). This lens is spherical and has the following characteristics properties: radius $a = 25$ µm, height $h = 6.25$ µm , radius of curvature $r = 53.1$ µm, focal length (at 632.8 nm) $f = 100$ µm, lens power $F = 0.62$ and a surface roughness $R_a = 40$nm.

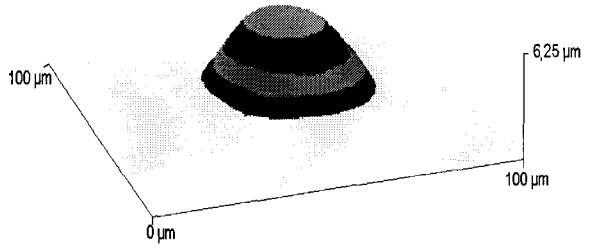

Fig 6: AFM micrograph of a lens obtained on a glass substrate with optimized ethanol content (30 wt.%)

In order to reduce the effect of the spreading of the sol having a higher ethanol content, lenses have been fabricated on a substrate whose interface has been coated with a thin layer (0.1 μm) of a low surface energy polymer. Figure 7 shows a fit of vertical cross section passing through the center of the lens by a semi circle, showing that the lense is practically spherical. This lens has the following properties: radius a = 37.5 μm, height h = 9 μm, radius of curvature r = 82.6 μm, focal length at 632.8 nm f= 125 μm, lens power F = 0.72, surface roughness R_a = 40 nm. 2-d intensity profiles of the light spot created at the focal plane by a collimated 632.8 nm laser beam traveling onto the substrate side of the lenses are shown in Fig. 8. Their shapes are practically Gaussian with a full width at half maximum (fwhm) equal to 1.8 μm and 6.2 μm respectively. These values are small and only slightly larger than those calculated for a diffraction limited lens of same dimensions (fwhm ~0.7 μm).

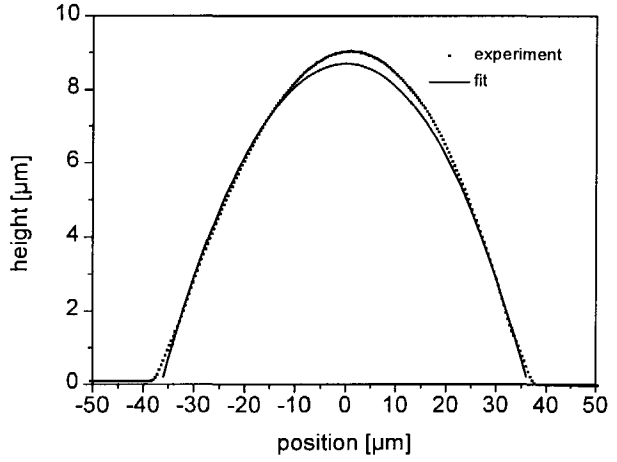

Fig. 7: Profilometer plot of the shape of a lens deposited on a modified glass substrate and fit of the vertical section by a semi circle

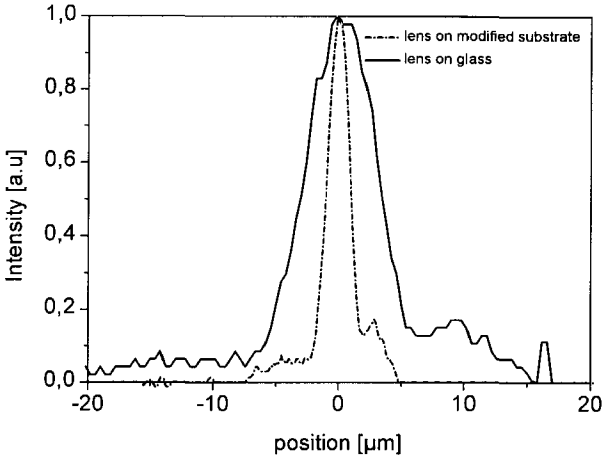

Fig. 8 Intensity profile of a light spot (l = 632 nm) measured the focal plane of the microlenses.

Reproducible arrays of hard, homogeneous, plano-convex microlenses have been obtained on fluorine modified glass substrates (Fig. 9).

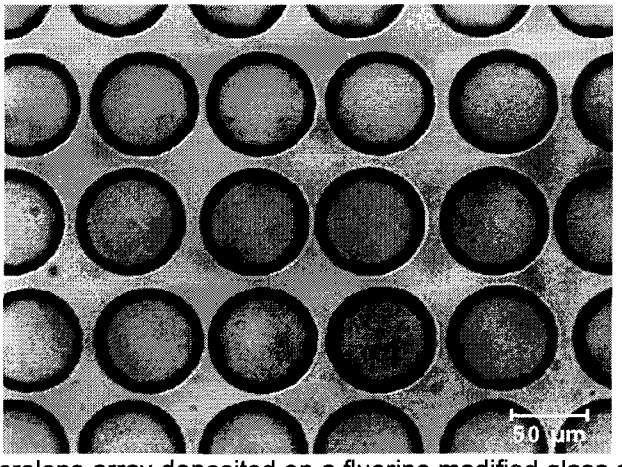

Fig. 9: Microlens array deposited on a fluorine modified glass substrate

Pad printing experiments were done with a commercial pad printer (Massek, PP21) using silicone tampons for transferring the sol from a steel cliché to a glass substrate. For these experiments the surface of the substrate was not modified by a polymer. A similar sol as for the ink-jet-printing prepared by

hydrolysis of MPTS was used. For the pad printing experiments no TEGDMA or UV-photoinitiator was added to the sol.

The sol prepared with a mol ratio MPTS: H_2O = 1:1.5 showed a dynamic viscosity h = 0.3 Pas after pre-hydrolyzing for 24 h at 40 C. With additions of different amounts of water and further hydrolyzing at 60°C for 4 h at every step, dynamic viscosities η up to 15 Pas were obtained. Lines and dots with diameters from 0.1-0.4 mm, etched 30 mm deep into a steel cliché were filled with the sol. After the printing process the coated substrate was heated at 200°C for 15 min.

Cylindrical and spherical lenses with good reproducibility have been printed. Figure 10 shows a 3-d plot of an array of 3 x 3 printed spherical lenses resulting from etched dots with 0.1 mm diameter in the cliché obtained with a sol having a viscosity h = 15 Pas. The lenses have diameters of ~0.2 mm indicating that the pad printing process leads to a broadening effect. This effect is strong for small structures (~0.1 mm) and for sols having a low viscosity but small for larger structures (> 0.3 mm) and sols having a high viscosity (> 10 Pas). Figure 11 shows a fit of a vertical cross section passing through the center of one of the printed lenses by a semi circle. The lens is practically spherical and has the following properties: radius a = 90 mm, height h = 4.2 mm, radius of curvature r = 0.95 mm, focal length f = 1.9 mm (assuming n = 1.5) and lens power F = 5.2.

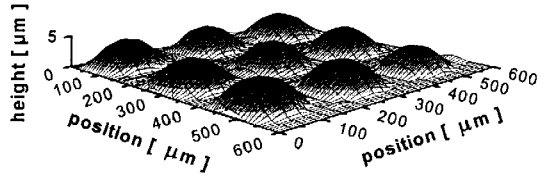

Fig. 10: Profilometer plot of an array of spherical microlenses with diameters of ~0.2 mm printed on a glass substrate

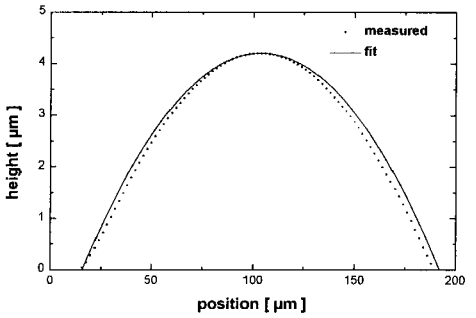

Fig. 11: Profilometer plot of the cross-section of one lof the ens of Fig. 6 and fit by a semi circle

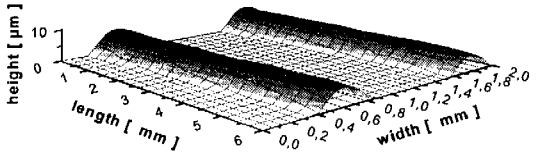

Fig. 12: Profilometer plot of two cylindrical lenses with 0.4 mm width printed on a glass substrate

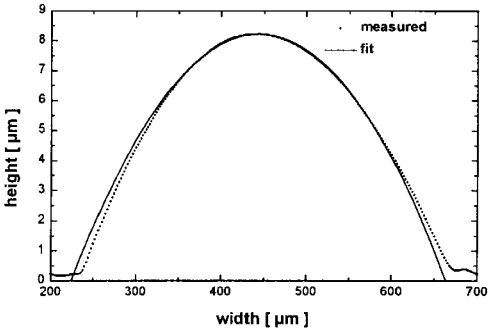

Fig. 13: Profilometer plot of the shape of a cylindrical lens from Fig. 12 and fit of the vertical cross section by a semi circle

Figure 12 shows a 3-d profilometer plot of two printed cylindrical lenses with widths of about 0.4 mm resulting from pad printing two etched lines of nearly the same widths in the cliché. The result shows that for structures of this size the pad printing process is able to transfer the etched structure in nearly identical size to the substrate. The shape of the lines corresponds to that of plano-convex cylindrical lenses. Figure 13 shows a profilometer plot of a vertical cross section and a fit of the shape by a circle. The lens has the

following properties: radius a = 220 mm, height h = 8.2 mm, radius of curvature r = 3 mm, focal length f = 6 mm (assuming n = 1.5) and lens power F = 6.3.

BIOMIMETIC PREPARATION OF HYDRATED TiO_2 THIN FILMS ON POLYCARBONATE

Film deposition on plastic substrates requires temperatures lower than 150 to 200°C. The conventional sol-gel process will lead to the formation of very porous and mechanically unstable layers. Wet chemical processes using hybrid materials where organics are incorporated into inorganic networks, are however better suited. Another possibility is provided by biomimetic processes which try to imitate biological systems [25]. Such methods are characterized by low process temperatures and moderate chemical environments. One approach in this field is the surface functionalisation, a technique which has already led to thin film synthesis of FeOOH, Fe_2O_3, SnO_2, CdS, $Al(OH)_3$ and TiO_2 [26].

The surface of a polycarbonate substrate (Makrolon 281, Röhm) can be sulfonated with a solution of SO_3 in H_2SO_4 and then etched by the formation of water soluble compounds. Hydrated TiO_2 coatings were then deposited from 0.05 M aqueous solution of $(NH_4)_2(OH)_2Ti(C_3H_4O_3)_2$ (Tyzor LA®, Dupont) and HCl in a Ti: HCl molar ratio of 1:1.95 by dipping the pretreated substrates into the heated solution (70°C) for 1 to 30 min. Figure 14 shows the variation of the film thickness as a function of the coating time. After a rapid growth, the thickness increases at a rate of 10 nm/min. 500 nm thick film has been obtained after 30 min.

X-ray diffraction measurements indicate that the layers are amorphous. The coatings are homogeneous, without cracks or islands (fig. 15), scratch resistant according to the tape test DIN 58196-K1, have an optical transmission in the visible range of ~ 82% with an index of refraction of ~ 1.9 at 550 nm and a probable composition of TiO_2 x H_2O. This process is therefore quite promising to coat thin oxide layers on polycarbonate substrates.

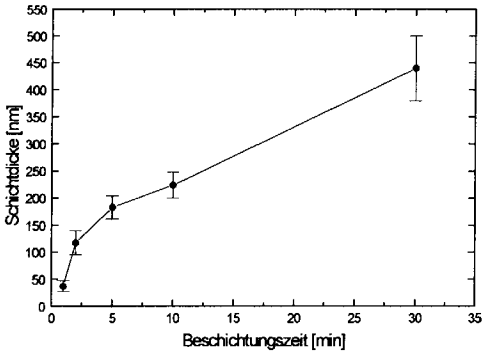

Figure 14: Thickness of the deposited TiO_2·x H_2O thin film on sulfonated polycarbonate vs. the coating time

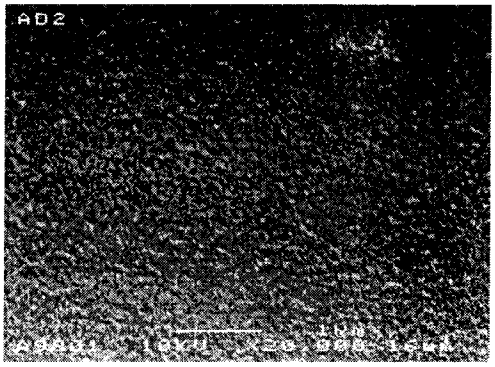

Figure 15: REM image of a TiO_2·x H2O coating on polycarbonate (30 min sulfonated, 10 min deposited)

FAST CO_2 LASER SINTERING OF SnO_2:Sb COATINGS

The sol-gel coatings obtained by dip or spin coating technique are usually dried and fired in two separate processes in a furnace. The heating and cooling which should be repeated to produce thick coatings are by far the speed-limiting factor of the coating process. An interesting technique using high power CO_2 laser whose radiation is absorbed by the glass substrate has been developed. It allows fast surface firing speed (up to 30 cm^2/s) of sol-gel layers up to temperature several hundred degrees higher than the Tg values of the glass substrates films.

The technique has been so far successfully tested for transparent conducting SnO_2:Sb coatings [9, 27]. Using a fast scan mode crack free coatings have been sintered at temperature as high as 1000°C obtained in a time as short as 0,1s (heating rate up to 4300 K/s). Laser firing was found to produce denser layers with larger crystallites than those fired in a furnace at the same temperature leading consequently to coatings showing lower resistivity. A comparison of the results obtained by both processes made for SnO_2:Sb coatings having an initial thickness after deposition of 158 nm and then

sintered at the same temperature (540°C) gives the following values: densitiy: 4,8 g cm^{-3} vs 3,2 g cm^{-3}, crystallite size: 12 nm vs 5 - 6 nm, sheet resistance 0.9 $K\Omega_{\square}$ vs. 4.4 $K\Omega_{\square}$, resistivity 8.5 10^{-3} Ωcm vs. 60 10--^{3} Ωcm. These correlated variations are thought to be due to a competition between nucleation at low temperature and the growth of the nuclei occurring at higher temperature. A low heating rate (0.2 K/s in a conventional furnace) leads to a low densification and favors a porous structure of small crystallites while a high heating rate (> 1000 K/s with the CO_2 laser) favors a denser structure built with larger crystallites and fewer pores.

ACKNOWLEDGMENT

The author thanks his colleages Dr. A. Mehrtens, D. Ganz, G. Gasparro, J. Pütz, C. Goebbert, S. Biehl, R. Danzebrink, R. Maschek, and A. Desouches for these research developments and BMBF (contract 2A67/03N9040) and the State of Saarland for financial support.

REFERENCES

[1] D. Burgard, C. Goebbert, R. Nass, „Synthesis of Nanocrystalline, redispersable antimony-doped SnO_2 particles for the preparation of conductive, transparent coatings“, *J. Sol-Gel Science and Technology*, in print

[2] C. Goebbert, M.A. Aegerter, „SnO_2:Sb coatings prepared from nanodispersed particles“, INM *Annual Report 1997*, in print

[3] C. Goebbert, M.A. Aegerter, „Influence of temperature treatment on BET surface, pore size and density of nanosized SnO_2:Sb particles“, *INM Annual Report 1997*, in print

[4] J. Pütz, M.A. Aegerter, „Spin-coating of MoS_2 thin films“, *these Proceedings*

[5] S. Biehl, R. Danzenbrink, M.A. Aegerter, „Refractive microlenses fabrication by ink-jet process“,. J. *Sol-Gel Science and Technology*, in print

[6] S. Biehl, R. Danzebrink, R. Maschek, A. Mehrtens, „Refractive microlenses fabrication by ink-jet and pad printing processes“, *these Proceedings*

[7] A. Dessouches, „Biomimetic TiO_2 thin Film Growth on Polycarbonate“, Diplom thesis Ecole Polytechnique (France) and INM (1997)

[8] A. Dessouches, J. Pütz, M.A. Aegerter, „Biomimetic preparation of TiO_2 thin films on polycarbonate“, *INM Annual Report 1997*, in print.

[9] G. Gasparro, D. Ganz, C. Goebbert, J. Pütz, M. A. Aegerter, „SnO_2:Sb transparent conducting coatings made by different sol-gel processes“, in Sol-Gel Optics IV, *SPIE* 3136, 407-418 (1997)

[10] D. Burghard, C. Kropf, R. Naß, H. Schmidt, „Routes to deagglomerated nanopowder by chemical synthesis,“ in Better Ceramics Through Chemistry, *MRS* 346, 101- 107 (1994)

[11] D. Burghard, R. Naß, H. Schmidt, „Aqueous Chemistry and Geochemistry of Oxides, Oxyhydroxides and related Materials“, in Better Ceramics Through Chemistry *MRS* 432, 113-120 (1997*)*

[12] G. Gasparro, D. Ganz, J. Pütz, M.A. Aegerter, „Multilayer SnO_2:Sb transparent electronic conducting coatings made by the sol-gel process“, these *Proceedings*

[13] H.L. Hartnagel, A.L. Dawer, A.K. Jain, C. Jagadish, in Semiconducting Transparent Thin Films, IOP Publishing, Bristol, 1995

[14] C. Goebbert, „Herstellung und Charakterisierung von transparenten, leitfähigen, Antimon-dotierten Zinnnoxid-Schichten aus nanodispersen Beschichtungssolen“, Diplom work, INM and University of Saarland, 1996.

[15] G.C. Chern and I. Lauks, "Spin-Coated Amorphous Chalcogenide Films", *Journal of Applied Physics,* 53 6979-82 (1982).

[16] T.A. Guiton and C.G. Pantano, "Sol-to-Gel and Gel-to-Glass Transitions in the As_2S_3-amine System", *MRS Proceedings 121*, 509-14 (1988).

[17] J.J. Santiago, M. Sano, M. Hamman and N. Chen, "Growth and Optical Characterization of Spin-Coated As_2S_3 Multilayer Thin Films", *Thin Solid Films,* 147 275-84 (1987).

[18] F.C. Eze, "Thin Films of Arsenic Selenide (As_2Se_3) Synthesized by Spin-Coating", *Physica B,* 160(3) 365-8 (1990).

[19] V. Buck, "Preparation and Properties of Different Types of Sputtered MoS_2 Films", *Wear,* 114, 263-274 (1987).

[20] M. Döring, „Ink-jet printing", *Philips Tech.,* 40, 192 (1982)

[21] A. Atkinson, J. Doorber, A. Hudd, D.L. Segal and P.J. White, „Continuous Ink-jet printing using sol-gel ceramic inks", *J. Sol-gel Science and Technology* ,8, 1093 (1997)

[22] S. Biehl, R. Danzebrink, P. Oliveira, M.A. Aegerter, „Refractive Microlenses Fabrication by Ink-jet Process", *Sol Gel Science and Technology*, in print

[23] D. Satas, "Pad printing" in Plastics Finishing and Decoration, D. Satas (ed.), Van Nostrand, Reinhold, 204 (1986)

[24] J. Bersin, R. Kasemann, G. Jonschker and H. Schmidt, „Easy-to-clean Beschichtungen von Einscheibensicherheitsglas (ESG)", *Annual Report INM*, 134 (1995)

[25] S. Mann, editor, Biomimetic Materials Chemistry, VCH Publishers, Inc (1996)

[26] H. Shin, R.J. Collins, M.R. DeGuire, A.H. Heuer, „Synthesis and characterization of TiO_2 Thin Films On Organic Self-Assembled Monolayers: Part I. Film Formation from Aqueous Solution" *J. Mater. Res.* 10, 692-698 (1995), „Part II: Film Formation via an organometallic Route", *J. Mater. Res. 10,* 699-703 (1995)

[27] D. Ganz, G. Gasparro, M.A. Aegerter, „Laser Sintering of SnO_2:Sb Sol-Gel COATINGS", *J. Sol-Gel Science and Technology*, in print.